DIMENSIONAL STABILITY IN SINGLE-FIRED POROUS TILE

by J.L. Amorós, A. Escardino, E. Sánchez, F Zaera.

Instituto de Tecnología Cerámica. Universitat Jaume I. Castellón.
Asociación de Investigación de las Industrias Cerámicas (AICE). Castellón. (España).

ABSTRACT

The appearance of wedging and differences in dimensions in production considerably reduces finished product quality. For large-sized ware, such as that at present being manufactured for wall tiling, variations in linear shrinkage of the order of 0.1% in the selfsame piece, give rise to wedging. Dilatometric analysis has shown that compositions used for single-fired porous tile shrink fast between 800 and 900°C. Wedging of the fired ware in many instances depends on this magnitude. In this study, the physico-chemical transformation responsible for this shrinkage is determined, as well as the effect of the different constituents of the body and the operating variables on this transformation.

1.- INTRODUCTION.

In order to achieve the high quality levels at present required in wall tiles, disposing not only of suitable compositions and appropriate processes but also of effective control systems is vital, to enable optimal values for the operating variables to be held within the preset margins. Both these aims can only be attained if the effect each of the composition constituents and each operating variable have on the most important finished property qualities, is thoroughly known beforehand. Dimensional stability (absence of wedging and differences in dimensions), is one of the most important characteristics of glazed ceramic wall tiles. For large-sized wall tiles (up to 400 mm), maintaining the required dimensional stability is often complicated, as variations of ±0.1% in linear shrinkage in the selfsame piece (wedging), or among the pieces (differences in sizes), are considered excessive.

In low porosity ceramic floor tile, and in general for those materials which undergo noticeable shrinkage variation with firing temperature and/or time, lack of dimensional stability in the finished product has experimentally been shown to be due to a lack uniformity in firing (in temperature or time), and/or lack of uniformity in porosity of the unfired ware (1). However, this explanation is unsatisfactory when it comes to interpreting these kinds of defects in porous wall tile, as these compositions, with high carbonate contents, hardly undergo firing shrinkage of over 1% and besides, variation of this property with firing temperature is virtually negligible (2).

2.- AIMS.

With a view to determining the reasons for the lack of stability found at times in porous single-fired wall tile, and to attempting to determine the possible influence starting composition and operating variables have on the appearance of these defects, a series of experiments was programed, made up of the following stages:

- Carrying out a set of experiments on a laboratory scale, modifying firing cycle and temperature profiles, in order to simulate the above-mentioned defect, whilst using industrial compositions.
- Establishing the nature of the physico-chemical transformation which can give rise to the appearance of these defects.
- Determining the influence the starting composition and the firing variables have on the physico-chemical transformation mentioned above.

3.- MATERIALS AND EXPERIMENTAL PROCEDURE.

3.1.- Materials.

In order to carry out this study, two spray-dried powders were used which are utilized industrially in single-fired porous wall tile manufacture. One of these, M, often used to give rise to problems related to dimensional stability; the other, B, behaved suitably. A common industrial spray-dried powder made from red clay (G), was used with a view to comparing behaviour of the foregoing two compositons (M and B) on firing, with that of compositions used in manufacturing low porosity floor tile. The chemical compositions, obtained by X-ray fluorescence, and the mineralogical species forming them, obtained by X-ray diffraction, are listed in Table I. Particle-size distribution of these industrial compositions was determined by laser diffraction (3) and is reported in Figure 1.

In order to dispose of compositions with varying amounts of the mineralogical species commonly making up industrial bodies, blends were prepared by using Araya clay (TA), quartz (Q), feldspar (F), and carbonate-free Araya clay (TAS). The last composition was prepared by treating Araya clay with an acetic acid solution (4). The chemico-mineralogical characteristics of these constituents are listed in Table II and their particle-size distribution is to be found in Figure 2.

3.2.- Experimental procedure.

3.2.1.- Preparation of the test pieces.

The synthetic compositions were prepared by mixing and homogenizing the raw materials in suitable proportions for 10 minutes in a laboratory ball mill with acetone. Cylindrical test pieces with a 5-cm diameter were shaped by pressing, at a pressing pressure of 25 MPa and a moisture content of 0.055 kg water/kg dry solid, from the powders obtained and from the industrial spray-dried powders. Dry bulk density was determined in all the test pieces by immersion in mercury (5).

3.2.2.- Thermal analyses.

Dilatometric analysis and differential thermal analysis (DTA), with a heating rate of 10°C/min, were utilized in studying the physico-chemical transformations which develop during firing.

	B (wt %)	M (wt %)	G (wt %)
SiO_2	59.30	55.90	60.70
Al_2O_3	14.30	15.20	17.40
Fe_2O_3	4.59	4.93	6.69
CaO	6.63	7.58	1.96
MgO	1.46	1.47	1.42
Na_2O	0.41	0.57	0.56
K_2O	3.01	2.97	3.33
TiO_2	0.63	0.67	0.80
P_2O_5	0.23	0.37	0.11
MnO	0.03	0.03	0.35
P.P.C.	9.36	10.27	6.60
Illite	XXX	XXX	XX
Kaolinite	XX	XX	XX
Quartz	XXXX	XXXX	XXXX
Feldspar	X	X	X
$CaCO_3$ (wt %)	10.9	12.0	3.1

Table I.- Chemico-mineralogical composition of the industrial compositions used.

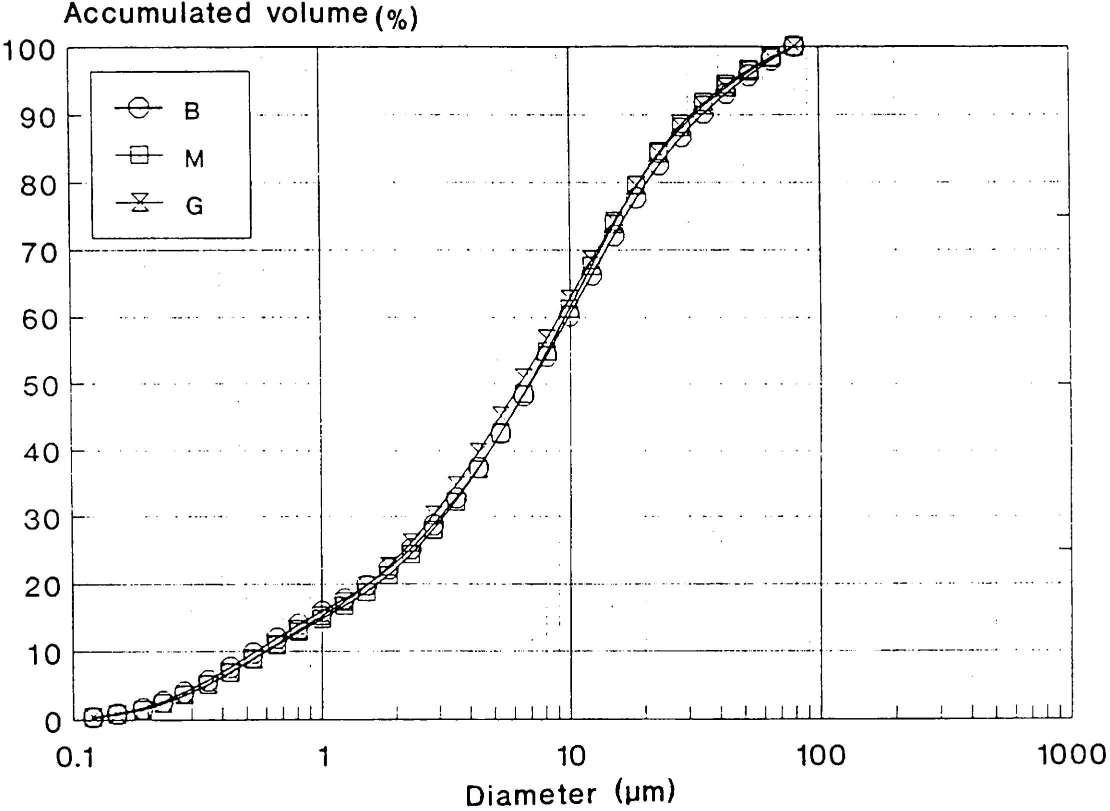

Figure 1.- Particle-size distributions of the industrial compositions.

	TA (wt %)	Q (wt %)	F (wt %)
SiO_2	33.20	98.60	65.10
Al_2O_3	13.20	0.72	19.10
Fe_2O_3	4.54	0.05	0.05
CaO	21.80	0.01	0.20
MgO	1.75	0.01	0.20
Na_2O	0.47	0.01	3.70
K_2O	2.90	0.17	11.20
TiO_2	0.45	0.06	<0.01
P_2O_5	0.23	<0.01	<0.01
MnO	0.04	<0.01	<0.01
P.P.C.	21.40	0.30	0.41
Illite	XXXX	--	--
Kaolinite	X	--	--
Quartz	XX	XXXX	--
Feldspar	--	--	XXXX
$CaCO_3$ (wt %)	36.1	--	--

Table II.- Chemico-mineralogical composition of the constituents used in formulating the laboratory compositions.

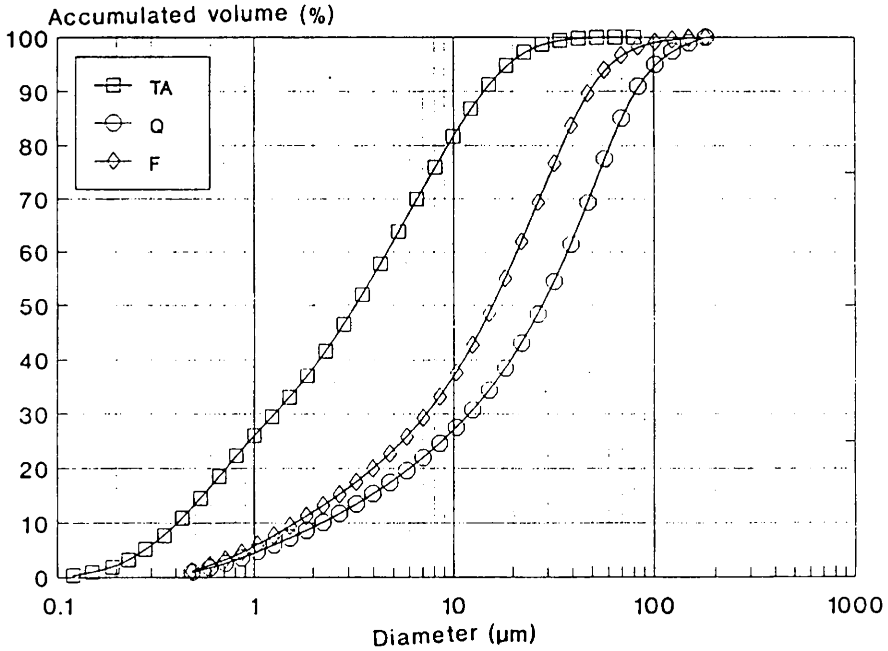

Figure 2.- Particle-size distributions of the constituents used in preparing the compositions.

3.2.3.- Fast firing in a laboratory kiln.

The procedure described below was followed to simulate the fast firing cycles commonly used in industry and to separately determine the effect of the preheating and firing stages on the dimensions and other properties of the fired ware (Figure 3). The previously dried test pieces were held for 30 min at 300°C, to make sure thermal equilibrium had been reached. The hot piece was then immediately set in a laboratory kiln at a temperature (Tp), and was then kept there for a certain dwell time (tp). After this period of time, the piece was then placed in a second kiln with a higher temperature (Tc), where it was also kept for a certain time (tc). The values of Tp, tp, Tc and tc were modified in each experiment. The values of the dimensions and bulk density were determined in all the test pieces.

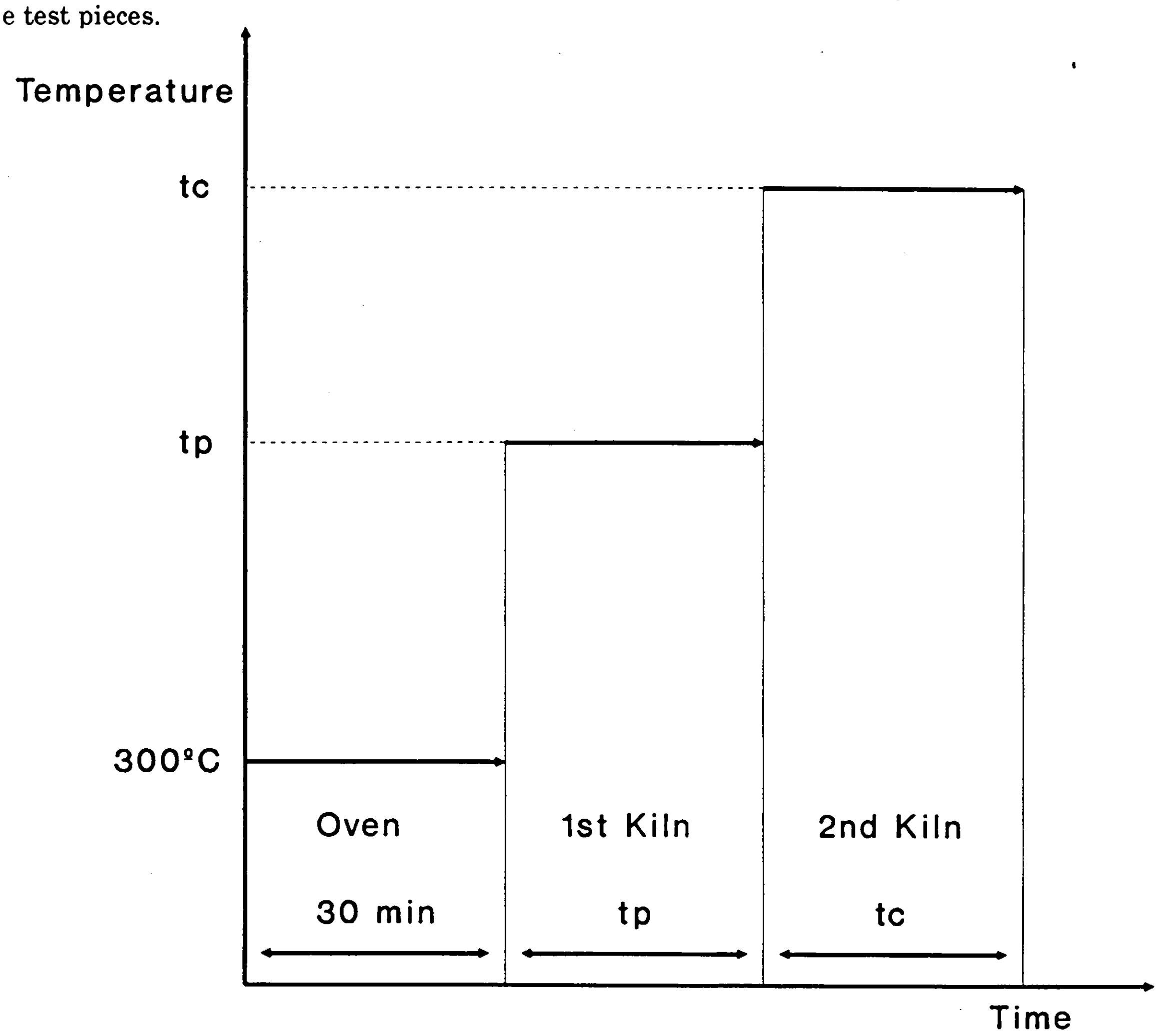

Figure 3.- Fast firing in a laboratory kiln

3.2.4.- Isothermal firing.

Isothermal firing experiments were run at different temperatures in an electric laboratory kiln, to study sintering and crystalline-phase formation kinetics at temperatures of interest. Just before setting the test pieces in the kiln, they were soaked for 30 minutes in another kiln at 725°C. By means of this treatment, breakdown reactions of the clay minerals were completed and most of the carbonates present were decomposed, without sintering of the test piece starting.

3.2.5.- Characterization of the fired test pieces.

In some of the test pieces, pore-size distribution and pore surface area were determined by mercury poresizing (6). Their microstructure was examined by scanning electron microscope (SEM). The determination of crystalline-phase formation and disappearance during firing was conducted by X-ray diffraction.

4.- RESULTS AND DISCUSSION.

4.1.- Laboratory-scale defect simulation. Likely cause of the defect.

In order to try and simulate lack of dimensional stability on a laboratory scale, as it is encountered at times in production, the following firing conditions were determined in works:

- Working cycle and single-layer kiln temperature profile.

- Thermal homogeneity in different sections of the kiln.

Furthermore, dimensions of the ware were measured on leaving the kiln in function of its position.

In Figure 4 the temperature values above and below the roller plane are reported, in function of the distance to the entrance of the ware to the kiln, and in function of dwell time of the ware. Temperature variation inside the kiln in function of distance to the wall for different kiln sections, was determined by means of a thermal sensor. Considerable difference between temperature at the kiln wall and temperature at the centre was only found in the preheating area. Figure 5 plots the temperature values near the kiln wall and at the centre, in function of the distance from the kiln entrance. The overall temperature profiles for the kiln sections S1, S2 and S3 in Figure 5 are reported in Figure 6.

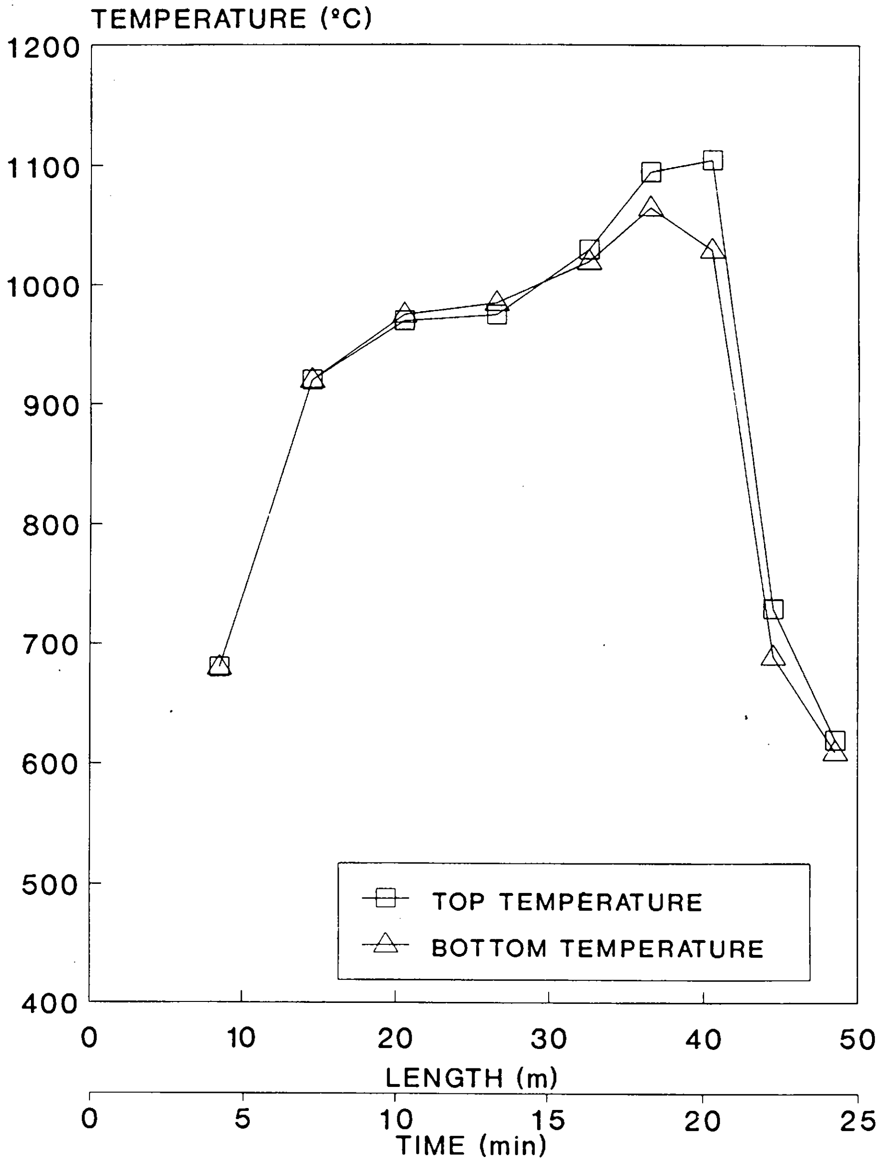

Figure 4.- Temperature profile of a single-layer kiln.

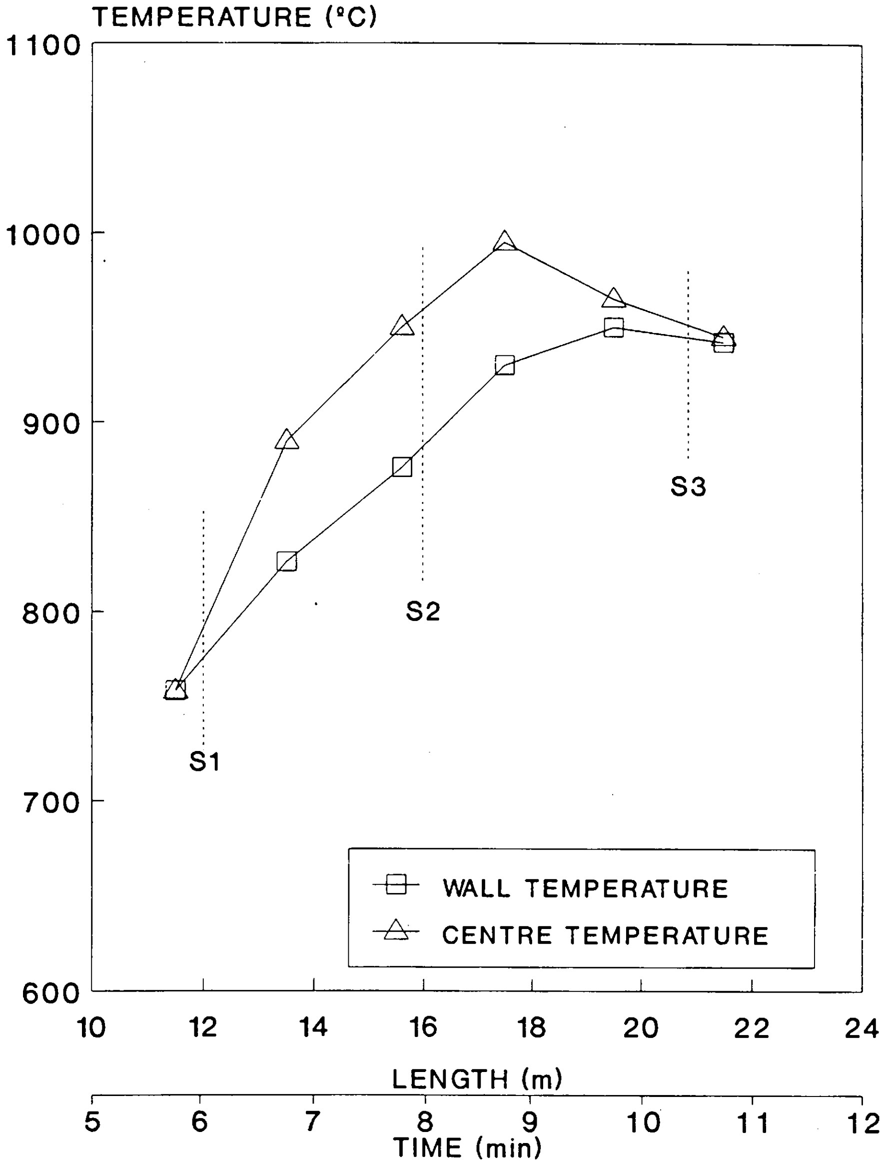

Figure 5.- Variation of kiln wall and kiln centre temperatures in function of the distance from the entrance.

With the kiln working in these conditions and using composition M, for pieces measuring 425x235 mm, wedging was only found in ware closest to the wall, whilst the side of the ware closest to the wall was clearly shown to be longer than the other (about 0.5 mm). On using composition B, although differences were found between the dimensions of the two longer sides of the piece, this magnitude was much less, so that these differences did not represent a defect.

These findings seem to indicate that temperature differences between the two sides of the ware during preheating could be the reason for this kind of wedging, since temperature uniformity in the firing area was very good. In order to verify this assumption, the effect of the preheating and the firing stages on final shrinkage, had to be independently determined. With this aim, a series of experiments was programed with compositions B and M, according to the procedure described in Section 3.2.3, suitably modifying temperature (Tp), and dwell time values (Tp), corresponding to preheating, and the values for Tc and tc corresponding to firing proper. In order to compare the behaviour of these compositions to those used in low porosity floor tile manufacture, some experiments of this kind were also run with composition G.

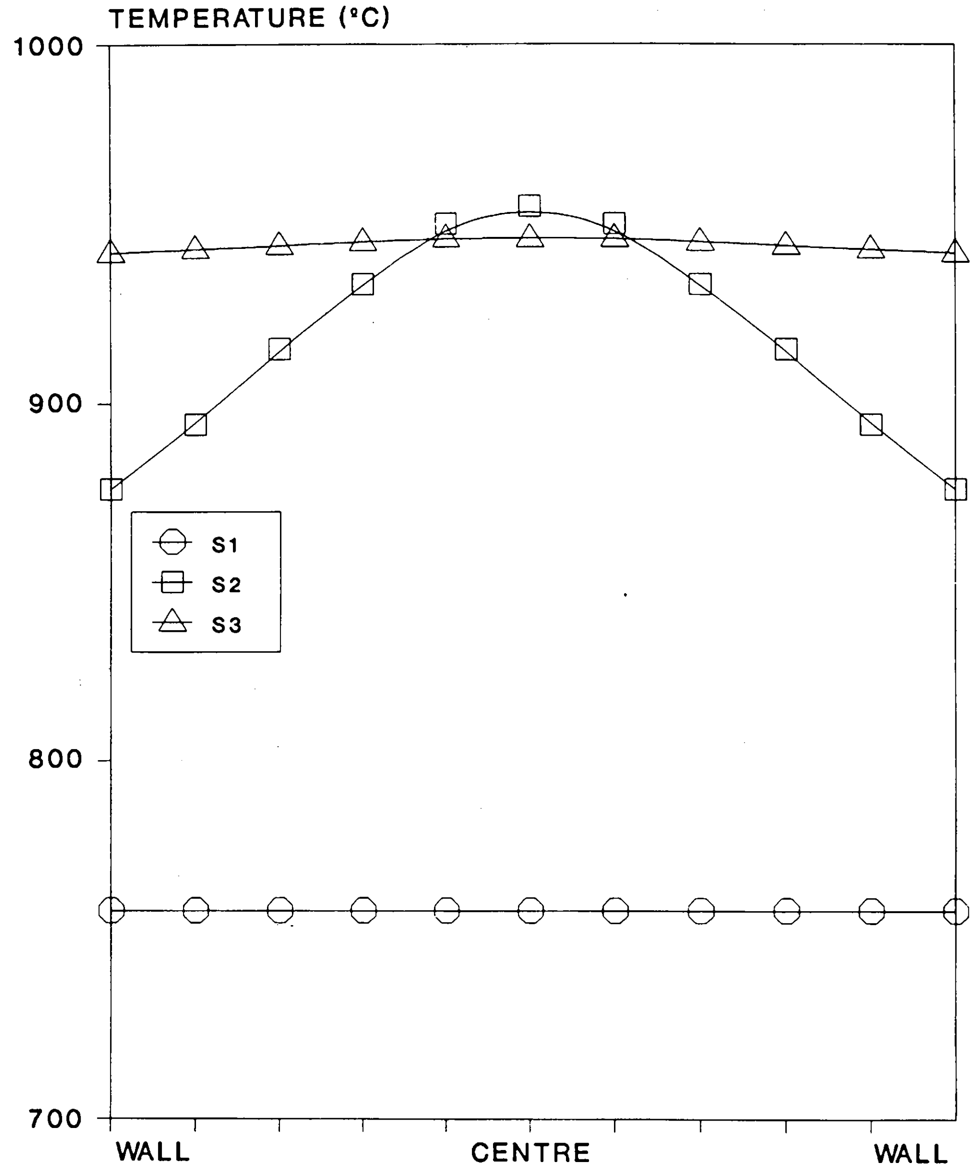

Figure 6.- Temperature profiles in the industrial kiln sections S1, S2 and S3 reported in Figure5.

The operating variables to be used in laboratory firing were chosen on the basis of industrial firing conditions. The values of the variables utilized as well as the firing shrinkage values obtained are listed in Table III.

On analyzing the findings the following may be observed:

- The values of linear firing shrinkage are observed to vary considerably with preheating temperature (Tp) and dwell time (tp) at this temperature, at the same firing temperature (Tc) and dwell time at this temperature (tc) for composition M, which showed wedging problems industrially. On the contrary these variations are virtually imperceptible for composition B which performed suitably on an industrial scale (Figure 7).

- On keeping preheating (Tp = 850°C and tp = 15 min) and firing temperature conditions (Tc = 1080°C) constant, the values of linear shrinkage corresponding to compositions M and B depend very slightly on dwell time at firing temperature (tc). This variation for composition B can even be seen to be a little greater than that for M, which is the composition with this problem (Figure 8).

Tp (°C)	tp (min.)	Tc (°C)	tc (min.)	Linear shrinkage B	M	G
800	2	1080	6	0.55	0.68	--
"	4	"	"	0.61	0.85	--
"	6	"	"	0.59	0.87	--
"	10	"	"	0.65	0.96	--
"	15	"	"	0.66	0.99	--
850	2	1080	6	0.58	0.82	3.76
"	4	"	"	0.58	0.93	3.87
"	6	"	"	0.61	1.00	3.90
"	10	"	"	0.71	1.23	3.97
"	15	"	"	0.82	1.38	3.97
900	2	1080	6	0.58	0.77	--
"	4	"	"	0.67	1.00	--
"	6	"	"	0.72	1.18	--
"	10	"	"	0.69	1.11	--
"	15	"	"	0.62	1.03	--
850	15	1080	3	0.73	1.28	3.31
"	"	"	6	0.82	1.38	3.91
"	"	"	9	0.86	1.38	4.47
"	"	"	12	0.93	1.42	4.49
850	15	1040	6	0.62	1.12	--
"	"	1060	"	0.76	1.21	--
"	"	1080	"	0.82	1.38	--

Table III.- Values of final firing shrinkage in function of the preheating and firing operating conditions.

- On modifying peak firing temperature (Tc), a slight variation in linear shrinkage, highly alike for both compositions, is observed with this variable.

These findings leave beyond doubt that the reason for the appearance of wedging in the fired pieces obtained from composition M, is the difference in shrinkage between the two sides of the selfsame piece, caused by temperature and/or time differences during preheating.

However, on determining the influence dwell time of the ware during preheating (tp) and firing (tc) has on the final shrinkage of the piece for the three compositions studied, it may be observed that unlike the compositions used in obtaining wall tiles (M and B), the stoneware compositions (7) are much more sensitive to the influence of dwell time at firing temperature (tc) (Figure 8). Contrariwise, the effect of dwell time in the preheating area (tp) on final firing shrinkage for composition G is virtually imperceptible, unlike what happens with some porous wall tile compositions such as M (Figure 9).

With the aim of attempting to justify the differing behaviour shown by these three compositions, their corresponding dilatometric curves were obtained (Figure 10). All firing shrinkage is observed to virtually take place between 800° and 925°C for the two porous single-fired wall tile compositions (B and M), owing to their high carbonate content. At higher temperatures the piece expands slightly and it only starts shrinking again at temperatures above 1050-1075°C. In the carbonate-free compositions or those with a low carbonate content however,like G, firing shrinkage develops progressively, allowing greater variation of this property to be observed with temperature as this variable increases.

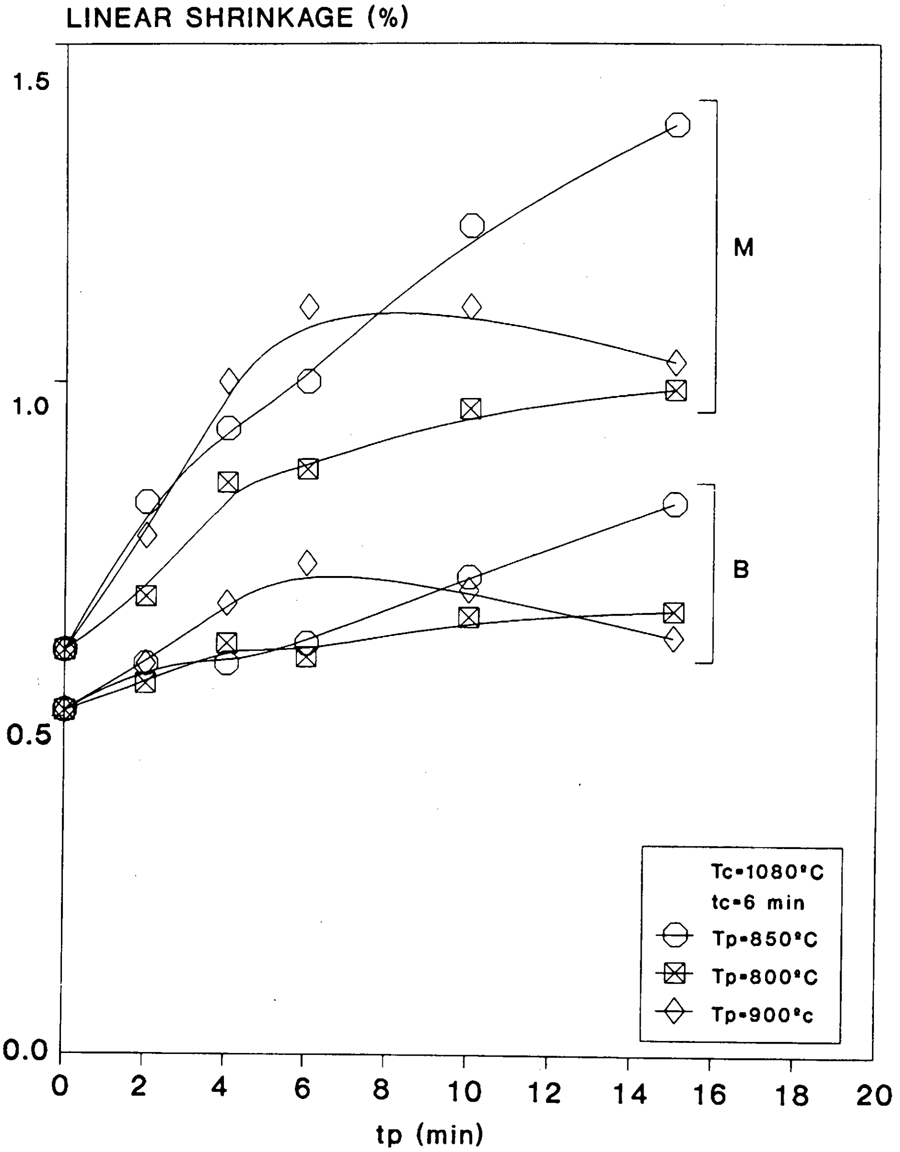

Figure 7.- Variation of final firing shrinkage in function of preheating temperature (Tp) and dwell time at this temperature.

On comparing these findings with those obtained in the above-mentioned fast firing experiments, a close relationship may be observed between the dilatometric behaviour of the unfired compositions and their behaviour during industrial firing. In fact, on comparing compositions M and B, composition M, which was most affected by changing preheating conditions of the ware, is seen to be just the one showing greater firing shrinkage between 800 and 925°C. Moreover, for both compositions, the effect of firing temperature (Tc) and/or dwell time at this temperature (tc) is virtually negligible, in accordance with the fact that variation in firing shrinkage with temperature for values ranging from 1000-1080°C is negligible. However, the opposite happens with floor tile composition (G). In fact, at normal firing temperatures, the variation in linear shrinkage with firing temperature is high, so that the influence of this variable (Tc) and/or dwell time (tc) at this temperature on linear shrinkage, will be considerable.

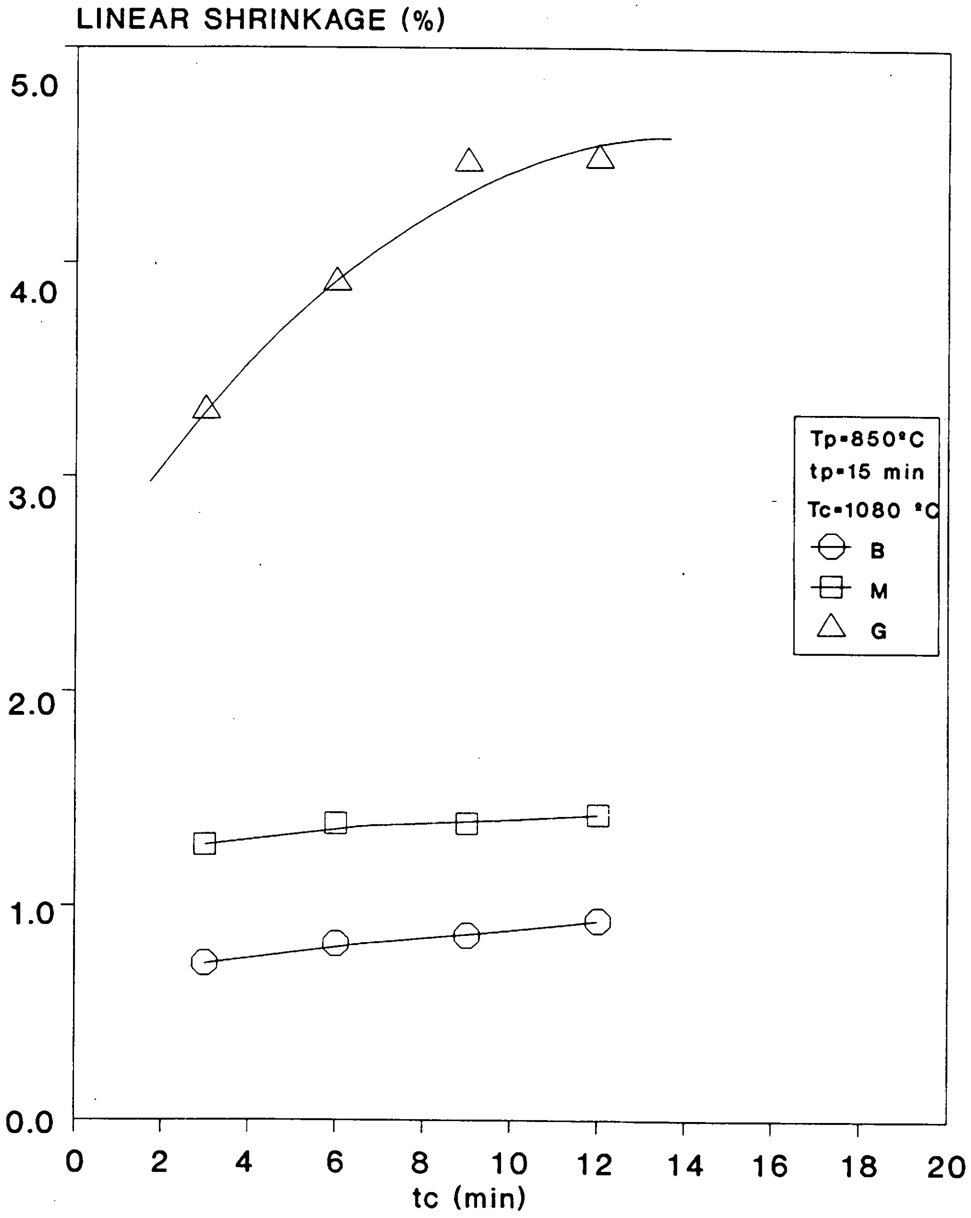

Figure 8.- Variation of final firing shrinkage in function of dwell time (tc) at firing temperature.

4.2.- Relation between the sharp shrinkage a composition shows at about 800°C and the effect that temperature and/or dwell time, to which a piece is subjected during preheating, have on final firing shrinkage. Influence of some body constituents.

In the foregoing section, a close, direct relationship was observed between the shrinkage the ware undergoes between 800 and 925°C when fired in a dilatometer, and the effect preheating temperature and time have on final shrinkage of the piece, in this temperature interval. In order to verify if this relationship is valid for other compositions and to determine the effect the most common body constituents have on this shrinkage, the compositions listed in Table IV were prepared.

Figure 11 reports a plot of the dilatometric curves corresponding to the four compositions listed in Table IV. They are all observed to show fast shrinkage between 800 and 925°C, and the greater the amount of calcium carbonate and the lower the amount of non-plastic material, the greater this magnitude is. In Figure 12, the variation of the values of the final firing shrinkage of the test piece are plotted for these four compositions, in function of dwell time (tp) at preheating temperature (Tp=850°C), while keeping the variables of the firing stage proper constant (Tc=1080°C and tc=6min).

On comparing the findings (Figure 12) obtained in fast firing experiments in a laboratory kiln (Section 3.2.3), to those found by means of dilatometric analysis (Figure 11), a close, direct relationship is to be observed between both results, just as on studying the industrial compositions. In fact, as the shrinkage value measured in the dilatometer increases at temperatures between 800-925°C, besides the final firing shrinkage, the effect that the preheating duration has on this characteristic of the fired piece increases. Analogous results were obtained by keeping dwell time of the piece constant during preheating (tp), and modifying the value of this temperature (Tp). As a result, it may be concluded for calcareous compositions, that final firing shrinkage of the ware and its tendency to produce size variations arising from changes in temperature and/or dwell time in the preheating area, are directly related to the magnitude of the shrinkage taking place in this kind of body between 800-925°C.

4.3.- Study of the physico-chemical transformation giving rise to sharp shrinkage of the ware between 800-900°C.

In the foregoing sections, all the compositions bearing a high percentage of $CaCO_3$ (over 10-12%) have been shown to characterize themselves by a similar dilatometric curve for the unfired piece (8, 9 and 10).

4.3.1.- Experiments at constant heating rate.

The following experiments were run with Araya TA clay, to study the set of physical and chemical transformations taking place during firing of this kind of composition, and specifically the one responsible for the sharp shrinkage mentioned above:

- Simultaneous thermal analysis (DTA-TG-DTG) of the composition.
- Dilatometric analysis of the unfired test piece.
- Firing the test pieces at different firing temperatures, to determine the evolution of the crystalline phases and its microstructure with this variable.

The findings from these experiments and their interpretation are summed up below:

1. At temperatures below 700°C, mainly oxidation reactions of the possible organic matter and breakdown of clay minerals and allotropic change of α-quartz to ß-quartz take place. All these transformations entail progressive increase in expansion of the piece (Figure 13), as well as porosity and specific surface area.

2. At temperatures close to 700°C, $CaCO_3$ decomposes releasing CO_2, which increases expansion of the piece, porosity and specific surface area even further. This highly endothermal reaction, lasts up to temperatures close to 800°C, as reported in Figure 14.

3. Fast sintering of the ware, virtually coinciding with the end of this reaction, takes place between 800-900°C, which is shown by a considerable increase in shrinkage (Figure 13) and by a parallel reduction in porosity and specific surface area. In this temperature interval, no crystalline-phase formation is detected. Similarly, it may be observed (Figure 13), that the rate at which this sintering takes place peaks at 860°C, which virtually coincides with an inversion point in the DTA curve, to be associated to calcareous crystalline-phase formation, which peaks at 890°C (Figure 14). It is therefore highly likely that this shrinkage is due to sintering of the amorphous phases arising from the breakdown of clay minerals and of CaO from $CaCO_3$.

4. At temperatures above 900°C, on continuing to heat the test piece, its size increases, owing to the progressive formation of gelenite and wollastonite. At the same time, pore size increases, virtually without modifying porosity of the piece.

4.3.2.- Isothermal experiments.

In order to determine the nature of the above-mentioned sintering process, a series of isothermal experiments was run (Section 3.2.4) at different temperatures, with Araya TA clay, in each case determining the variation with time of the firing shrinkage, the crystalline phases present, the specific surface area and loss on ignition.

The findings are listed in Figures 15 to 21. On analyzing these results the following may be concluded:

1. The sintering process of the ware is observed to partially overlap the decomposition reaction for all the tested temperatures of the calcite, which was not completely removed during the preliminary heat treatment at 725°C (Figure 17).

2. On comparing Figures 15 and 16, the considerable increase in shrinkage at reduced firing times is seen to correspond to a decrease of the same magnitude in internal pore surface area. This indicates that virtually all small-sized pores, mainly formed by the breakdown of clay minerals and calcite, are removed during sintering.

3. Continuous increase in linear shrinkage with thermal treatment time, is only observed for the piece treated at 800°C (Figure 15). This is due to calcic-phase formation being very small at this temperature (Figure 18). However, a clearer drop may be observed in the shrinkage rate for times over 100 min, which corresponds to gelenite formation (Figure 18).

4. Except for temperature at 800°C, variation of linear shrinkage with thermal treatment time peaks at each temperature (Figure 15). At longer firing times, shrinkage of the ware decreases, owing to the considerable formation of calcic phases (Figs. 19, 20 and 21).

5. Furthermore, Figure 15 shows that the value of final shrinkage corresponding to each temperature increases with the value of this variable up to about 850°C. At higher temperatures, final firing shrinkage is lower.

The behaviour shown by this kind of composition during sintering is due to the rate at which this process develops being conditioned by two simultaneous, antagonistic effects, which depend to a large extent on temperature. On the one hand, on increasing temperature, apparent viscosity of the amorphous phases decreases, which tends to raise the sintering rate. On the other hand, on increasing the value of this variable, the amount of amorphous phases drops as the crystallization rate of the calcic phase rises, which tends to reduce the sintering rate. The outcome of these two opposing effects leads to peaking of both the variation in linear shrinkage with temperature, as well as its variation with time for temperatures over 800°C.

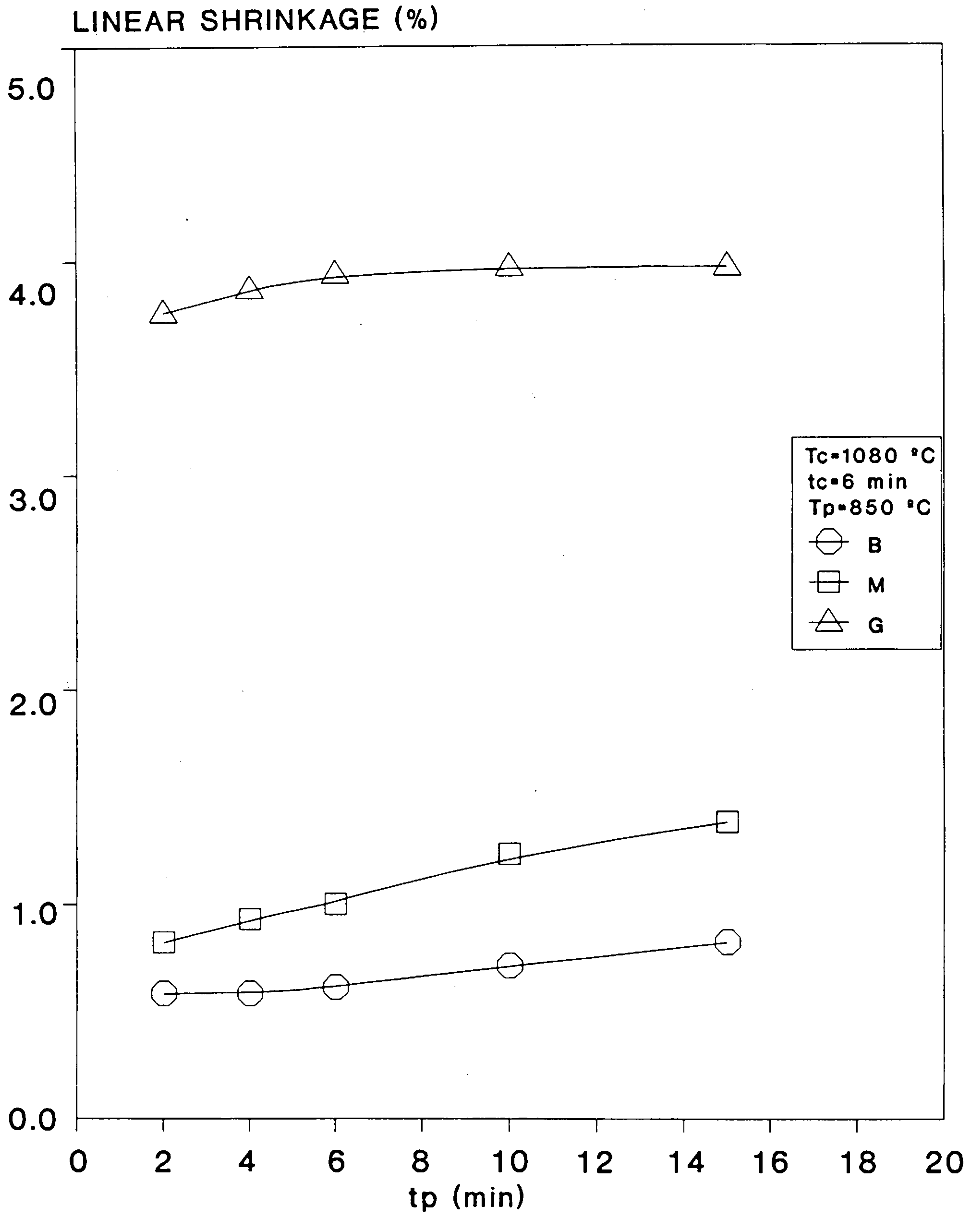

Figure 9.- Variation of final firing shrinkage in function of dwell time (tp) at preheating temperature (Tp).

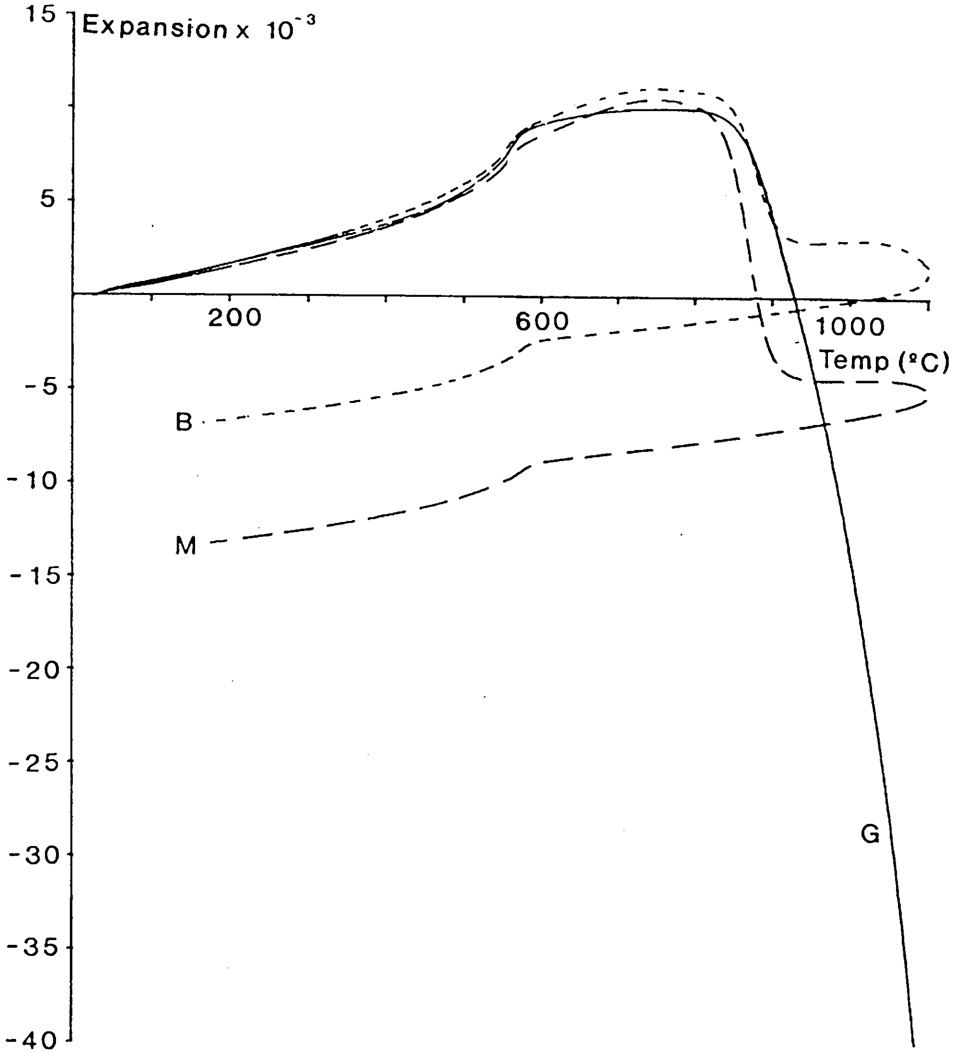

Figure 10.- Dilatometric curves of compositions B, M and G.

Constituent	TA (wt %)	TA15 (wt %)	TAQ (wt %)	TAF (wt %)
Araya Clay (TA)	100	41.5	41.5	41.5
Carbonate-free Araya clay (TAS)		58.5	28.5	28.5
Quartz			30	
Potassium feldspar				30
$CaCO_3$	36.1	15.0	15.0	15.0

Table IV.- Compositions prepared in the laboratory.

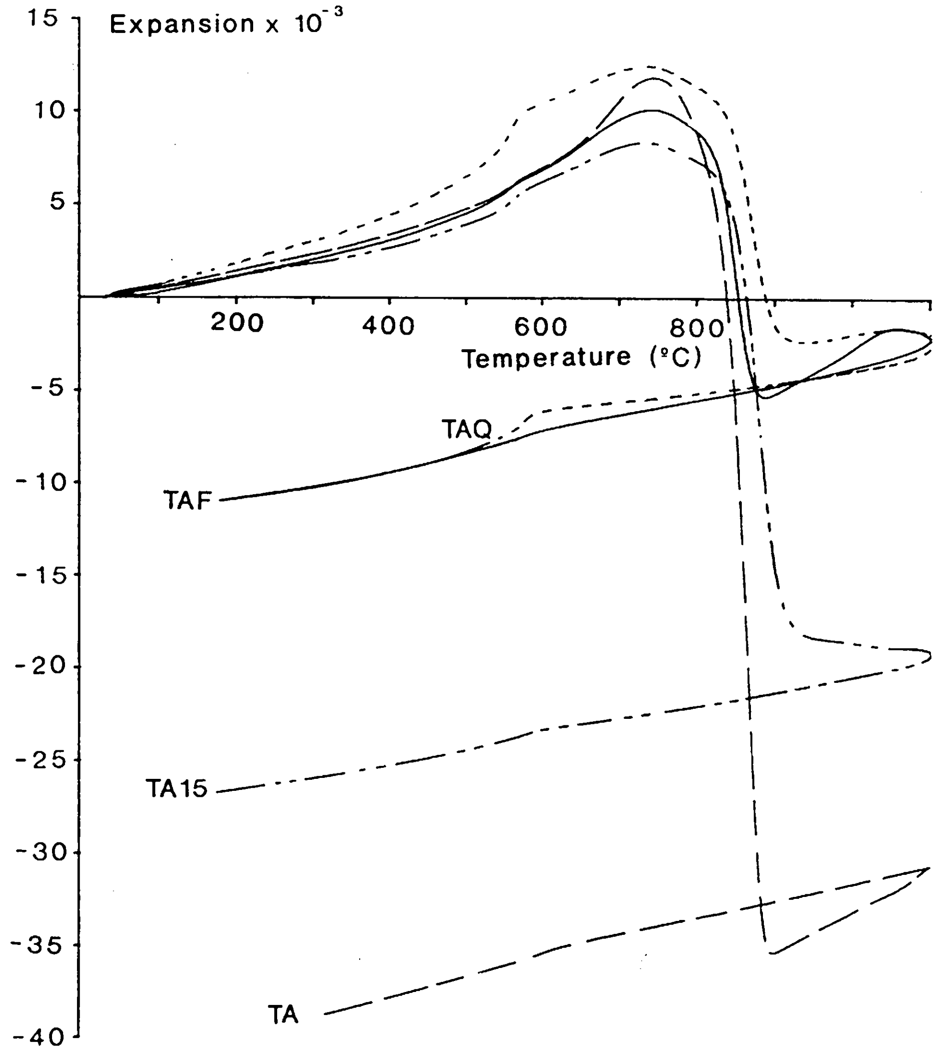

Figure 11.- Dilatometric curves of compositions TA, TA15, TAQ and TAF.

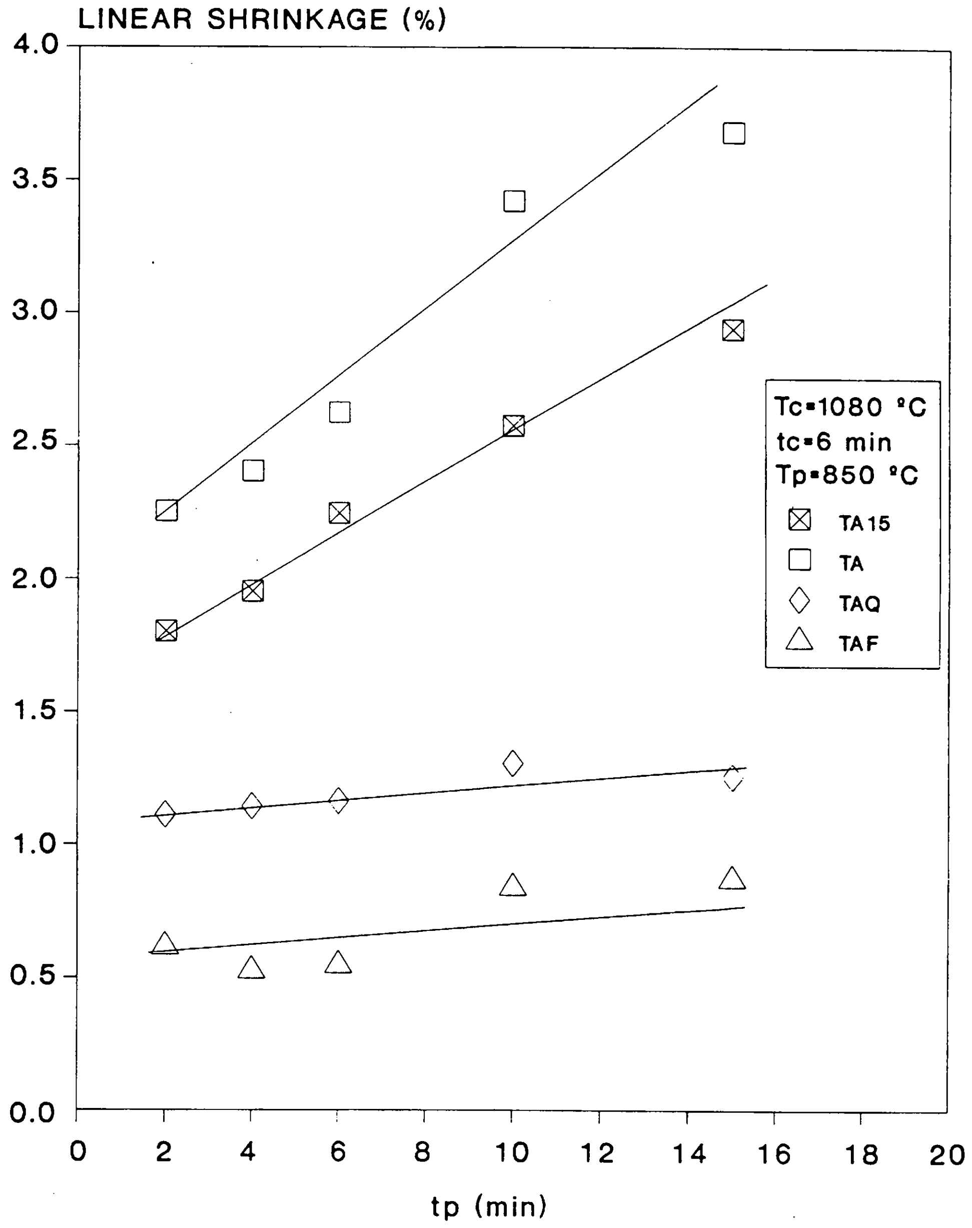

Figure 12.- Variation of final firing shrinkage with dwell time (tp) at preheating temperature (Tp).

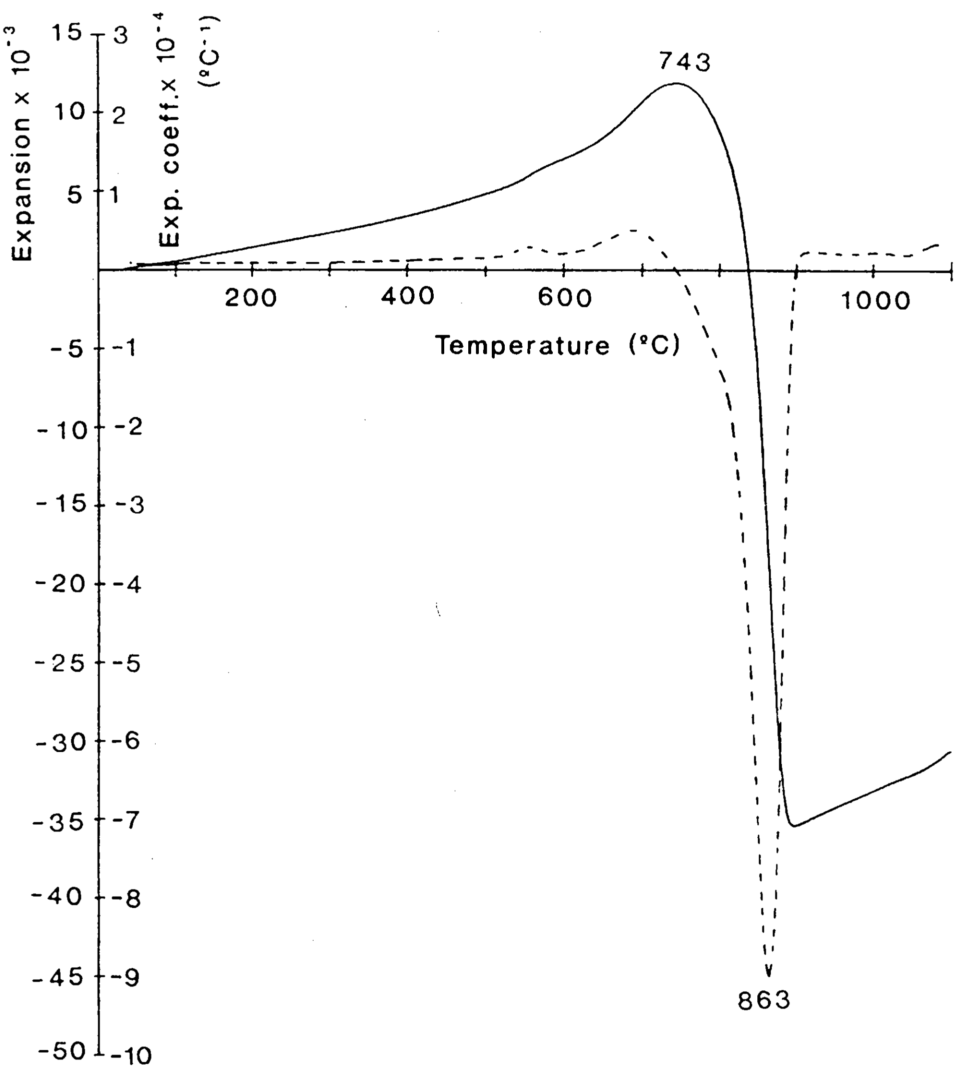

Figure 13.- Dilatometric curves of TA clay.

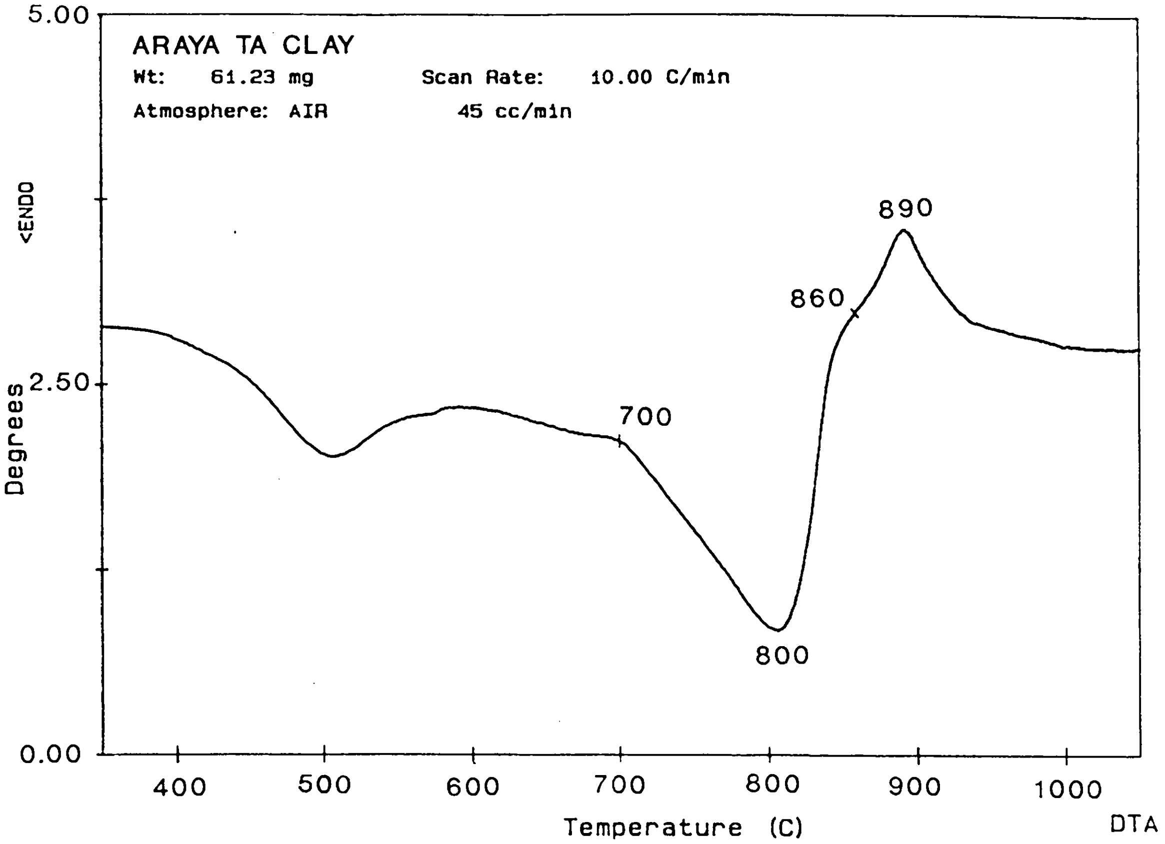

Figure 14.- Differential thermal analysis of TA clay.

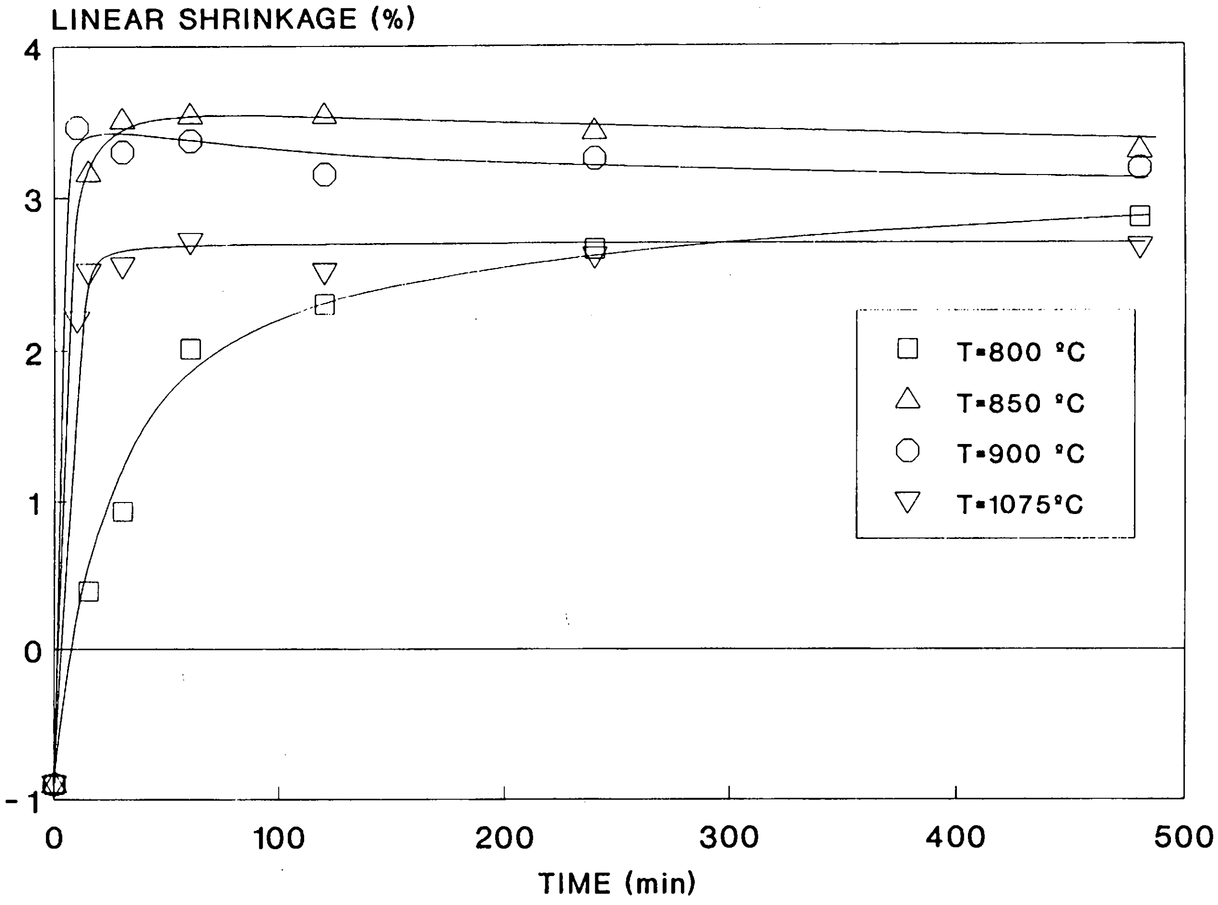

Figure 15.- Variation of linear shrinkage with dwell time at different temperatures.

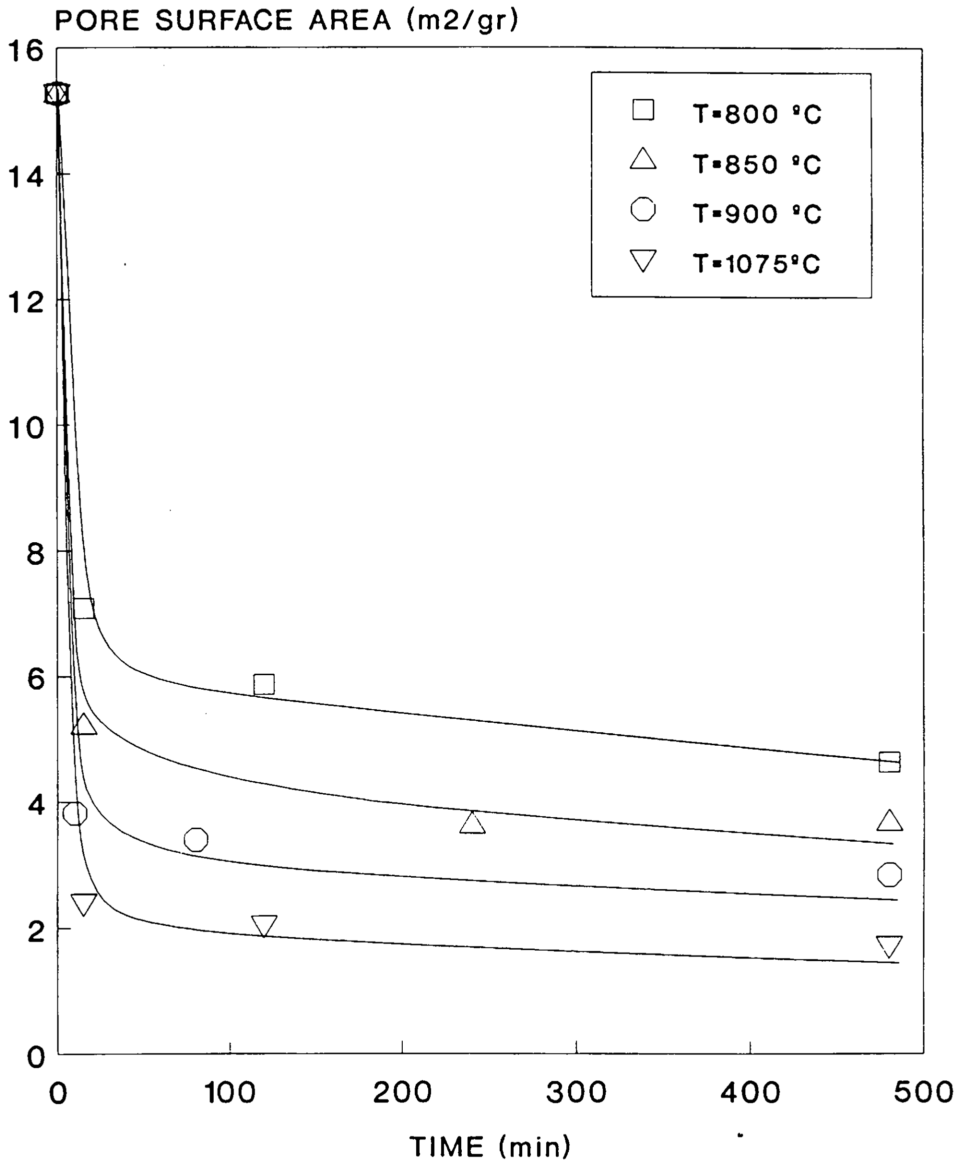

Figure 16.- Variation of pore surface area with dwell time at different temperatures.

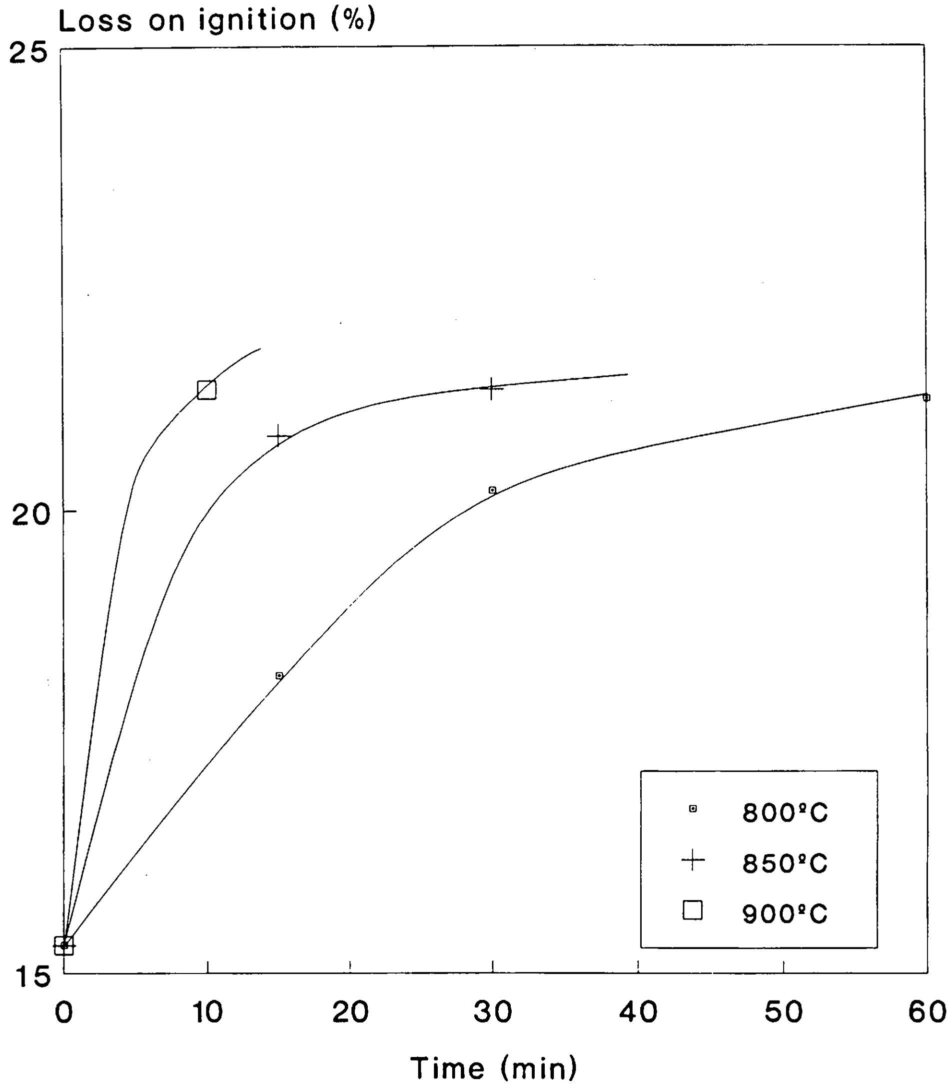

Figure 17.- Variation of loss on ignition with temperature and isothermal treatment time.

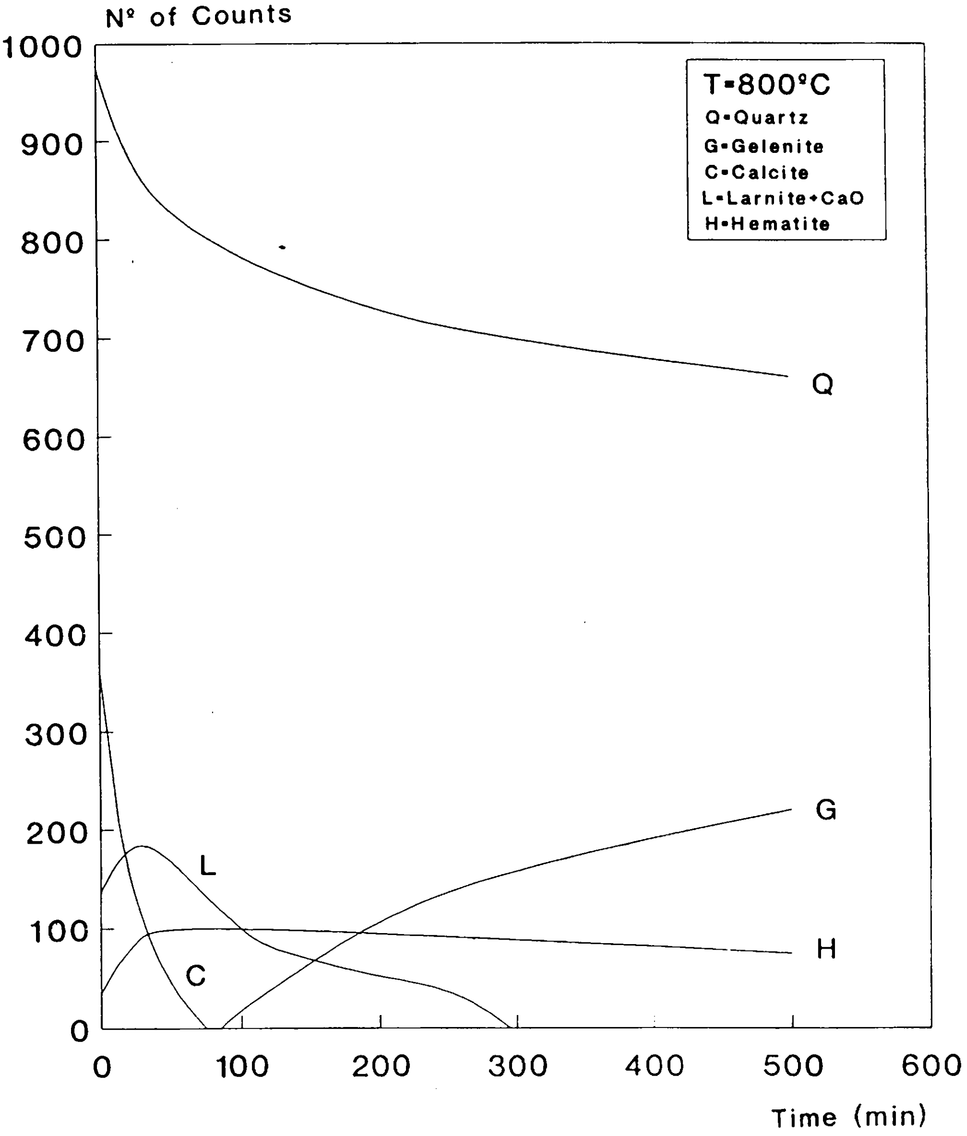

Figure 18.- Crystalline-phase evolution with dwell time at 800°C.

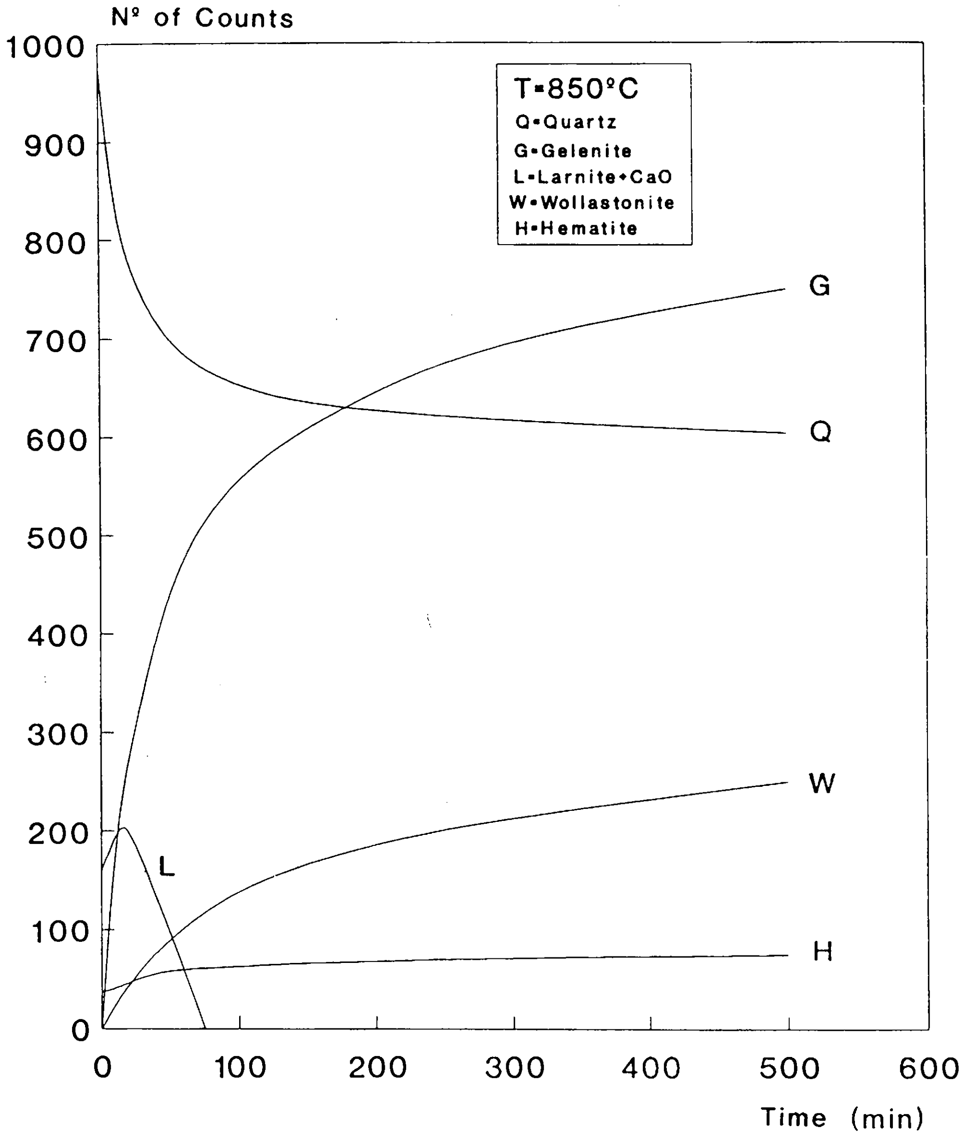

Figure 19.- Crystalline-phase evolution with dwell time at 850°C.

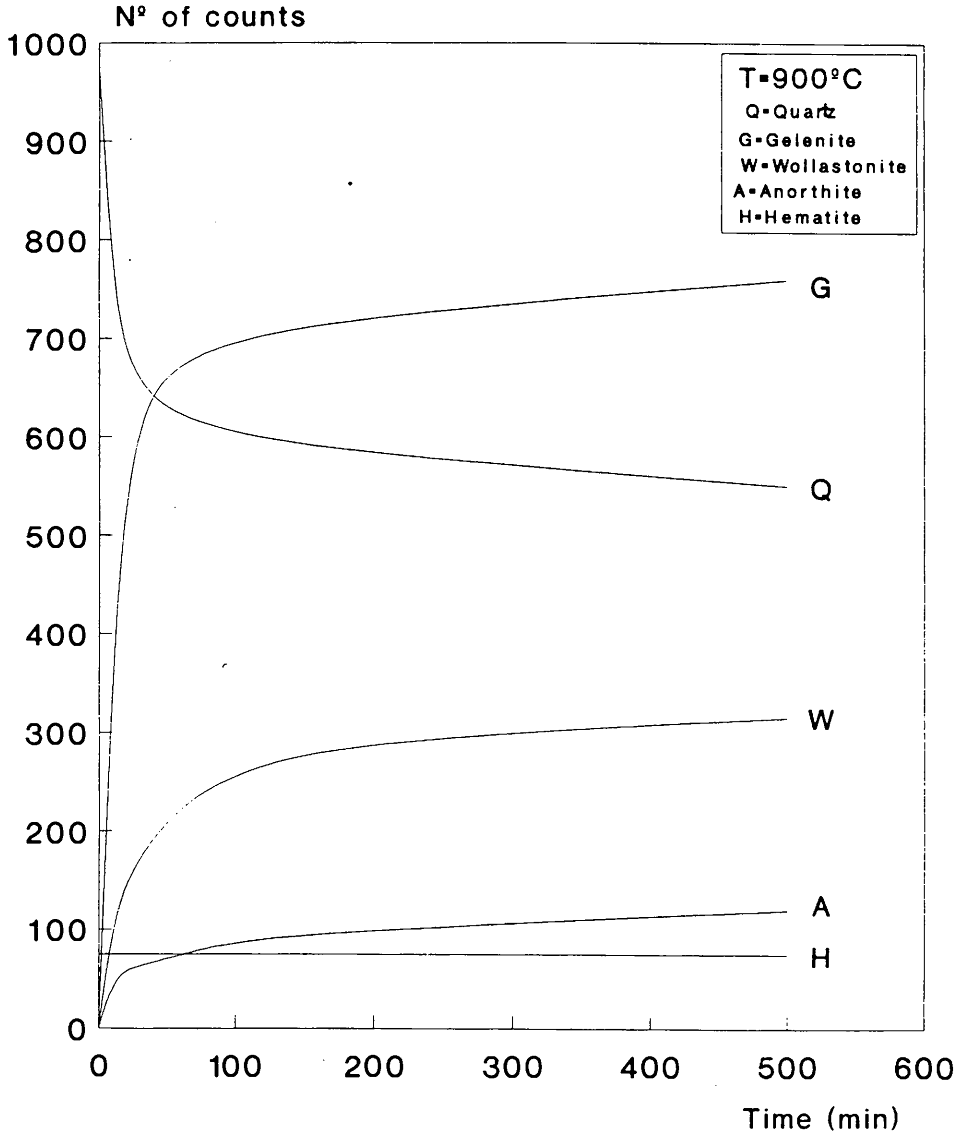

Figure 20.- Crystalline-phase evolution with dwell time at 900°C.

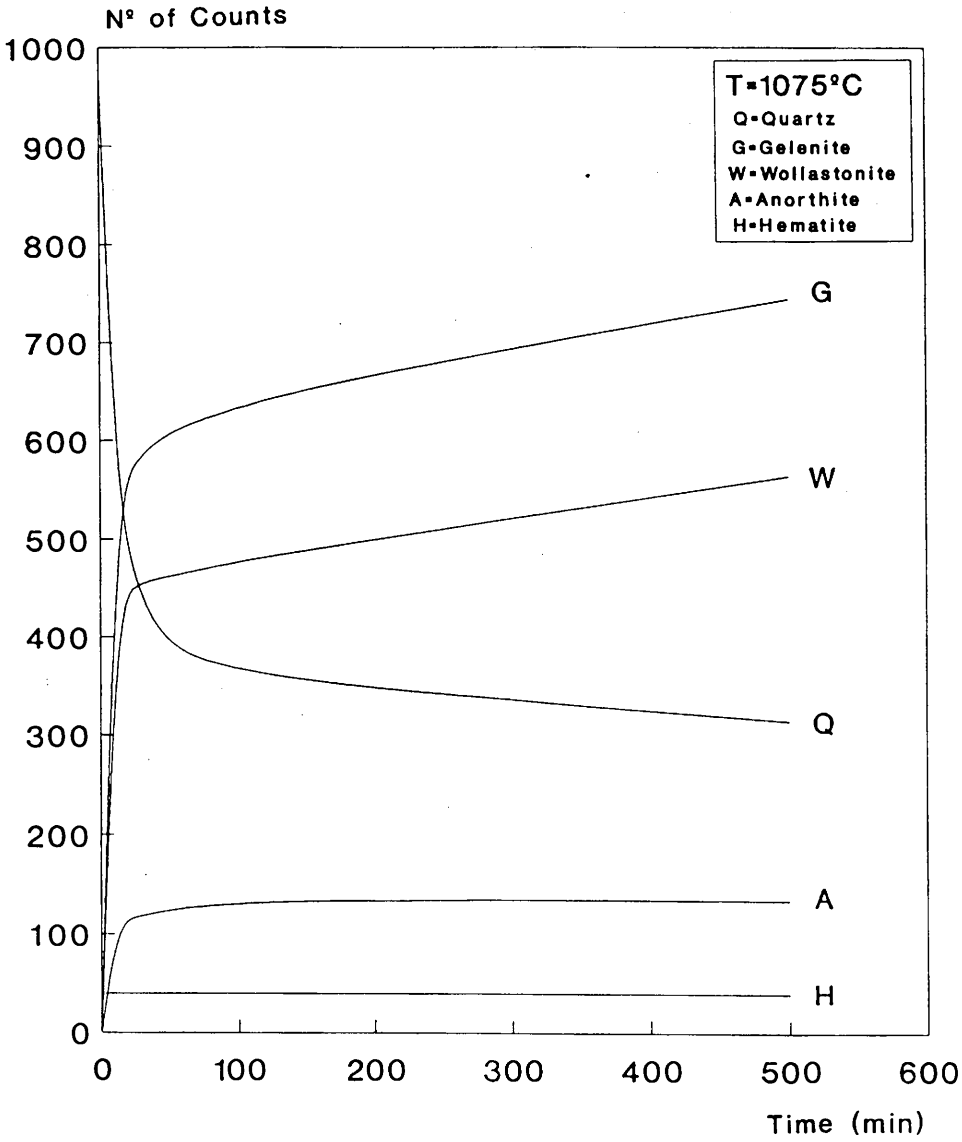

Figure 21.- Crystalline-phase evolution with dwell time at 1075°C.

5.- CONCLUSIONS.

- An experimental procedure was set up enabling the effect which the preheating and the firing stage have independently on the final shrinkage of the fired ware, to be determined.

- It was shown on a laboratory scale, that the reason for the appearance of wedging in fired ware, obtained from high carbonate-bearing compositions, was the difference in shrinkage the two sides of one selfsame piece undergo, caused by a difference in temperature and/or dwell time of the ware in the preheating area.

- Final shrinkage of the ware and the tendency to show variations in size, because of alterations in temperature and/or dwell time in the preheating area (appearance of wedging), for compositions with $CaCO_3$ contents over 10%, were shown to be directly related to the shrinkage value which develops in this kind of body, in the 800-925°C range. Determination of the fast shrinking the piece undergoes at about 800°C, by means of dilatometric analysis, is the most suitable procedure for controlling and optimizing a single-fired porous tile composition, as far as defects regarding dimensional stability are concerned.

- The magnitude of this shrinkage was shown to be greater in accordance with higher calcium carbonate content and lower amounts of non-plastic materials.

- The physico-chemical transformation responsible for the sharp shrinkage pointed out above, was shown to be sintering of amorphous phases from the breakdown of clay minerals and of CaO from calcite.

6. REFERENCES.

1. Amorós J.L.; Escardino A.; Beltrán V.; Enrique J.E.
Técnica Cerámica, 118, 1307-1314, 1983.

2. Enrique J.E.; Amorós J.L.
Técnica Cerámica, 91, 119-130, 1981.

3. Wertheimer A.L.; Wilcock, W.L.
Appl. Opt., 15, 1616 (1976).

4. Maniatis Y. et al.
J. Am. Ceram. Soc. 66(11), 773-781 (1983).

5. Amorós J.L.; Beltrán V.; Blasco A.; Felíu C.; Sancho Tello M.
Técnica Cerámica 116, 1234-1246, 1983.

6. Shahinpoor M. "Advances in the mechanics and the flow of glanular materials. Volume 1"
Edit., Trans. Tech. Publications, New York (1983).

7. Escardino A.; Amorós J.L.; Enrique J.E.
Bol. Soc. Esp. Ceram. Vidr. 20 (1), 17-24, 1981.

8. West R.
J. Can. Ceram. Soc. 34, 29-33 (1965).

9. Cizeron G.
L'Industrie Ceramique, 795(6), 405-410 (1985).

10. Peters T.; Iberg R.
Ceram. Bull., 57(5), 503-509, (1978).